Melting of inclusions with variable vacancy contents

1991 J. Phys.: Condens. Matter 3 5621

(http://iopscience.iop.org/0953-8984/3/29/015)

J. Phys.: Condens. Matter 3 (1991) 5621–5637. Printed in the UK

Melting of inclusions with variable vacancy contents

E V Kholopov
Institute of Inorganic Chemistry of the Siberian Division of the Academy of Sciences of the USSR, 630090 Novosibirsk, USSR

Received 27 November 1990

Abstract. The development of a model considered earlier, which deals with the melting of microinclusions in an elastic matrix, is proposed. Apart from perfect inclusions totally filling the appropriate cavities, inclusions with one atomic vacancy in the solid state are also described. The consideration is based on the exactly soluble model of a phase transition that describes two-level systems connected to a medium by a ferroelastic interaction. Some principally new types of phase diagrams with critical points where the lines of first-order phase transitions terminate are discussed. Peculiar regions of the model parameters are pointed out. As anticipated, the present results are applicable to a rather wide class of materials composed of several sets of distinct two-level systems.

1. Introduction

In the last few years, composites have been the subject of intense interest owing to the synthesis of different modern artificial compounds. In particular, zeolite matrices, in which there are regularly distributed cavities filled with some distinct material, can be regarded as important representatives of the discussed materials [1]. Melting is one instructive physical phenomenon in these compounds. A specific character of melting occurs in the case when every separate inclusion is sufficiently small that the coexistence of different phases is impossible within one, though such an inclusion consists of several atoms. A significantly richer picture of the corresponding thermodynamic behaviour is anticipated if some additional premelting states of the inclusions exist [2, 3]. In this case, apart from the prediction that the single line of the first-order phase transition terminates at the critical point, the splitting of that line leading to the appearance of an intermediate phase can be expected.

In the present paper another natural situation for the discussed system of microinclusions has been studied. Here we deal with the possibility of the existence of defective inclusions composed of a smaller number of atoms. All the cavities containing inclusions are assumed to be identical here. For definiteness, throughout this paper we restrict ourselves to a system of spherical cavities, every one of which may contain eight spherical atoms packed in a cubic configuration. In this case a defective inclusion consists of seven atoms that are packed in the same manner, i.e. the seven atoms are distributed over the eight positions of the perfect configuration. Such ordered states of the inclusions are naturally treated in the same way as their solid states. The unoccupied atomic position in a solid defective inclusion can then be regarded as a vacancy. The overall concentration of such vacancies in a specimen is assumed to be fixed. We believe that such a requirement

0953-8984/91/295621 + 17 $03.50

corresponds to the experimental situation and is determined by the conditions governing the synthesis of an appropriate sample.

According to [2, 3], the process of melting is associated with the transition of an inclusion to a state of high mobility, which is characterized by some atomic configuration with a larger number of unoccupied effective atomic positions. For example, such a state can be achieved by the transition of one atom belonging to a given inclusion to the central position in the corresponding cavity [2, 3]. Then the other atoms fill the volume of the spherical layer between the central atom and the boundary of the cavity, provided that there is an appropriate decrease in the atomic sizes. The fact that the total number of atoms persists within every cavity naturally leads to a significantly larger amount of empty volume per atom in a cavity after such a transformation. As a result, high atomic mobility is typical there. Moreover, now inclusions are described by different total energies and by different degrees of degeneracy of both the solid and liquid states depending on the presence of vacancies.

It seems to be important that the introduced system can be regarded as a new type of composite solid solution, namely a solution of inclusions embedded in an elastic host matrix. The present paper is devoted to the investigation of the thermodynamic peculiarities of such a solution.

2. States of a single inclusion

According to [3], the solid state of a perfect inclusion inserted into a spherical cavity of an elastic matrix is represented as a cubic cluster of eight atoms. An important assumption in what follows is that all the atoms of such a cluster are in intimate contact with one another and with the surface of the cavity, so that there is transmission of possible inner stresses to the outer medium and vice versa.

As far as both the shape and size of the involved clusters are concerned, they agree with the experiments of [1]. In particular, the experimental number of atomic positions is equal to $m_s = 8$ and corresponds to the number of atoms in a perfect inclusion.

The liquid state is in turn described by a configuration of the atomic positions such that one atom is located at the centre of the cavity and the other atoms are distributed at random around the central one, provided that all the constituent atoms are deformed identically. This variant of the atomic rearrangement is akin to the idea of transferring atoms to interstices. The essential distinction from the latter in its classical form consists of the fact that the entire rearrangement is accompanied by changing the environment, and therefore its character is local and collective simultaneously. Note that the extension of this approach to the description of bulk melting [4] gives rise to a new qualitative understanding of the melting phenomenon as a whole.

To calculate the total number m_l of admissible atomic positions of the liquid configuration, we directly make use of the geometric picture shown in figure 1. Then the close packing of atoms in the cavity can be obtained as follows. Three atomic positions along the vertical axis are assumed to be fixed, whereas the side spherical atoms can move independently along two parallel rings whose planes are normal to the above vertical axis. If we now consider one of the parallels of latitude at which the centres of the side atoms reside, then the length of this parallel divided by the length of the arc of the same parallel corresponding to the atom in question (this arc is restricted by the

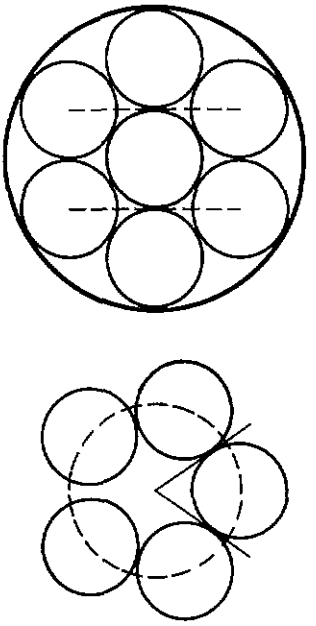

Figure 1. Model configuration of admissible atomic positions (small circles) for the liquid state in a spherical cavity. The central cross section is shown in the upper part. Side positions are distributed concentrically around the axis. The parallels of latitude on which the centres of those atoms reside are shown by broken lines. In the lower part the configuration of side atomic positions is given on the plane of the above parallel. The arc of that parallel restricted by the indicated angle corresponds to a single atomic position and is used for calculating m_l.

angle shown in the lower part of figure 1) yields the number of positions in each ring. On taking account of both the contribution of the two rings and the three fixed positions mentioned above, we easily derive $m_l \approx 13.2086$.

The atomic configurations introduced above specify both the states of a perfect inclusion with number of atoms equal to $n = 8$ and the states of an inclusion with a vacancy, when $n = 7$. Inasmuch as all the atoms within an inclusion are treated as identical, the degree of degeneracy of the solid state is determined by the obvious expression

$$q_{sn} = \frac{m_s!}{n!(m_s - n)!} = \begin{cases} 1 & \text{at } n = 8 \\ 8 & \text{at } n = 7. \end{cases} \tag{1}$$

To obtain the appropriate relationship for the degrees of degeneracy of the liquid states, the fact that the central atomic position is always occupied must be taken into account. This circumstance leads to some distinction from the model of bulk melting [4], though its effect on the final results is not appreciable. An exhaustive count of all the possible configurations describing the arrangements of atoms over admissible atomic positions gives rise to the formula

$$q_{ln} = \frac{\Gamma(m_l)}{(n-1)!\,\Gamma(m_l - n + 1)} = \begin{cases} 937.69 & \text{at } n = 8 \\ 1057.22 & \text{at } n = 7. \end{cases} \tag{2}$$

Here the relationship $\Gamma(m + 1) = m\Gamma(m)$, which holds for the gamma function $\Gamma(m)$, is used. The large numerical values of q_{ln} are typical for the present model.

Inasmuch as every given inclusion is specified by the two states, it is convenient to describe it as a two-level system with the help of an Ising variable $\eta = \pm 1$, where the upper and lower signs correspond to the liquid and solid states, respectively. In order to

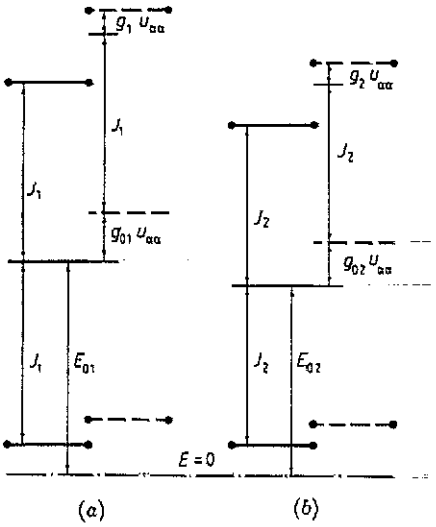

Figure 2. Energy parameters of the Hamiltonian H^{inc} on the diagram of two-level states of the (*a*) perfect and (*b*) defective inclusions. Both the upper (liquid state) and lower (solid state) levels are labelled by filled circles. The lines without a label are the midpoints. The chain line at the bottom gives the common origin. Broken lines show the appropriate shift of the picture due to some deformation.

distinguish the two types of inclusions, we introduce one more Ising variable $\psi = \pm 1$, where the upper sign describes an inclusion with a vacancy whereas the lower sign relates to a perfect inclusion. The projection operators on the states with and without a vacancy can be written respectively in the form

$$\Lambda_1 = \tfrac{1}{2}(1 - \psi) \qquad \Lambda_2 = \tfrac{1}{2}(1 + \psi).$$

Then the Hamiltonian of a single inclusion can be represented as follows:

$$H^{inc} = \sum_{j=1}^{2} [E_{0j} + g_{0j} u_{\alpha\alpha} + (J_j + g_j u_{\alpha\alpha})\eta]\Lambda_j. \tag{3}$$

The meanings of the appropriate energy parameters are specified by the scheme shown in figure 2. In particular, E_{0j} are the midpoints between the energy levels of the appropriate two-level systems labelled by j, and the corresponding energy gaps between the levels are equal to $2J_j$. The terms with $u_{\alpha\alpha}$ in expression (3) describe respectively the dependences of E_{0j} and J_j on the local change in volume of a cavity. The latter is determined as usual by the trace of the local strain tensor $u_{\alpha\beta}$ of the elastic matrix at the location of a given cavity. Here and below summation over repeated tensor indices is supposed.

As far as the values of the energy parameters of formula (3) are concerned, they can be associated with the deformation energy of spherical atoms upon their transformation to the liquid state. The accuracy of such an approximation is sufficient for the problem in question. The entire energy of an inclusion is then treated as the sum of contributions of the constituent atoms. The energy of any additional interatomic interaction is assumed to be a small correction to the above energy of deformation of the atomic electron shells, which is huge in comparison with typical excitation energies in solids. This circumstance enables us to neglect such additional contributions in what follows. As a result, some simple model relations between the parameters of formula (3) can be established:

$$J_1 = 4E_a \qquad g_1 = 4(g_{al} - g_{as}) \qquad J_2/J_1 = g_2/g_1 = \tfrac{7}{8} \tag{4}$$

where E_a is the energy of the deformed liquid state of an atom, provided that the energy

of the undeformed atom is set equal to zero, and g_{al} and g_{as} are the stiffness coefficients of an atom in the liquid and solid states, respectively, measured in energy units. Similarly, the connections between E_{01} and E_{02} and between g_{01} and g_{02} can be established within the framework of the additional assumption that the energies of the solid states for both sorts of inclusions coincide at $u_{\alpha\alpha} = 0$. Then

$$E_{0j} = J_j \qquad g_{01} = 4(g_{al} + g_{as}) = \tfrac{8}{7} g_{02}. \tag{5}$$

It is also natural to suppose that

$$g_{al} > g_{as} > 0$$

inasmuch as an atom in a compressed state is obviously stiffer. Furthermore, an increase in the local volume of the matrix leads to the contraction of cavities.

3. Thermodynamic potential

Now we consider a system of the above inclusions distributed regularly in an elastic matrix, which, for simplicity, is assumed to be isotropic. The appropriate Hamiltonian is of the form

$$H = \sum_i H_i^{inc} + \int (\tfrac{1}{2}\lambda u_{\alpha\alpha}^2 + \mu u_{\alpha\beta}^2)\, dV. \tag{6}$$

Here the summation is carried out over all N inclusions. The Hamiltonian H_i^{inc} is given by expression (3) with parameters η_i, $\Lambda_{j,i}$ and $u_{\alpha\alpha}(r_i)$ specifying the state of the ith inclusion. The second term in (6) corresponds to the elastic energy of the matrix in the continuum approximation [5], λ and μ are the elastic moduli, and integration is carried out over the volume V of the sample at hand. It is convenient in what follows to separate the interaction with the strain. According to (4) and (5), it can be written in the form

$$H_{int} = \sum_i g_1 \xi_i u_{\alpha\alpha}(r_i) \tag{7}$$

where

$$\xi_i = \tfrac{1}{16}(15 - \psi_i)(t + \eta_i) \tag{8}$$

is the effective order parameter specifying the state of the ith inclusion, and $t = g_{01}/g_1$. After detaching interaction (7), the residual part of the Hamiltonian describing only the system of inclusions is as follows:

$$H_{inc} = \tfrac{1}{16} J_1 \sum_i (1 + \eta_i)(15 - \psi_i).$$

Within the framework of the present approach, all the inclusions are described identically, though the presence of vacancies distinguishes them. In other words, our system of inclusions can be treated as a uniform one. As a result, it is natural to describe this system in terms of a grand canonical ensemble of inclusions, provided that the distribution of vacancies is not fixed. Such a representation is especially convenient at the stage of separating the elastic degrees of freedom upon calculating the partition

function. The appropriate thermodynamic potential is of the form

$$\Omega = -T \ln \mathrm{Tr} \left\{ \exp \left[-\beta \left(H + \sigma \sum_i \Lambda_{2,i} + p \int u_{\alpha\alpha} \, \mathrm{d}V \right) \right] \right\} \tag{9}$$

where $T = 1/\beta$ is the temperature measured in energy units, p is the external pressure, the trace is taken over both the configurations of the inclusions and the configurations of the elastic degrees of freedom, and σ is the chemical potential determining the concentration c of defective inclusions. The value of c is easily specified by the condition

$$\partial\Omega/\partial\sigma = Nc. \tag{10}$$

The homogeneity of the overall system, enables us to describe the system in terms of Fourier transforms. The appropriate consideration for an interaction similar to (7) is proposed in [6] (see also [3]). Separation of the regular contribution of harmonic phonons from the thermodynamic potential is performed with the help of the results of [7]. Then expression (9) can be converted into the form

$$\Omega = \Omega_0 + \tfrac{1}{2}N\sigma + \tfrac{1}{2}NG\langle\xi\rangle^2 - T \ln \mathrm{Tr} \left[\exp \left(\beta \sum_i \{ J\xi_i + \tfrac{1}{256}R[226t\eta_i - 15\psi_i(t^2 + 1 + 2t\eta_i)] + \tfrac{1}{16}(1-t)J_1\psi_i - \tfrac{1}{2}\sigma\psi_i \} \right) \right] \tag{11}$$

where

$$\Omega_0 = \Phi_a - p^2V/2K - \tfrac{113}{256}NR(1 + t^2) + \tfrac{15}{16}N(1 - t)J_1 \tag{12}$$

$$G = \frac{g_1^2}{v}\left(\frac{1}{K} - \frac{1}{\lambda + 2\mu}\right) \tag{13}$$

$$R = \frac{g_1^2}{v(\lambda + 2\mu)} \tag{14}$$

$$J = g_1 p/K - J_1 + G\langle\xi\rangle \tag{15}$$

Φ_a is the thermodynamic potential of acoustic phonons, $v = V/N$, $K = \lambda + 2\mu/3$, the trace in formula (11) is taken over all the admissible configurations of only the system of inclusions, and the value of $\langle\xi\rangle$ is determined by the condition that Ω be a minimum. The appearance of additional terms in expression (11) in comparison with formula (11) of [6] is associated with the fact that, according to definition (8), we have

$$\xi_i^2 = \tfrac{1}{128}(113 - 15\psi_i)(t^2 + 1 + 2t\eta_i). \tag{16}$$

Hence, the value of ξ_i^2 contains both operator terms and purely numerical ones. To obtain relationship (16), we have made use of the obvious condition on the Ising variables:

$$\eta_i^2 = 1 \qquad \psi_i^2 = 1.$$

In order to calculate the trace in formula (11), we rewrite the corresponding expression in the form

$$\mathrm{Tr} \left[\exp \left(\beta \sum_i [A\xi_i - B\eta_i + (D - \tfrac{1}{2}\sigma)\psi_i] \right) \right] = I^N \tag{17}$$

where

$$A = J + \tfrac{15}{8}U \qquad B = \tfrac{7}{8}U \qquad D = \tfrac{15}{256}R(t^2 - 1) + \tfrac{1}{16}(1 - t)J_1$$

and $U = tR$. Summing over the values of η_i and ψ_i in formula (17) is performed directly. As a result, we obtain

$$I = q_{17}\exp\{\beta[\tfrac{7}{8}(t+1)A - B + D - \tfrac{1}{2}\sigma]\} + q_{s7}\exp\{\beta[\tfrac{7}{8}(t-1)A + B + D - \tfrac{1}{2}\sigma]\} + q_{18}\exp\{\beta[(t+1)A - B - D + \tfrac{1}{2}\sigma]\} + q_{s8}\exp\{\beta[(t-1)A + B - D + \tfrac{1}{2}\sigma]\}. \tag{18}$$

The first two terms on the right-hand side of (18) can be converted to a single term, and the last two terms are transformed in the same manner, so that formula (18) is rewritten as follows:

$$I = 2\{Q_7\exp[\beta(D - \tfrac{1}{2}\sigma)] + Q_8\exp[-\beta(D - \tfrac{1}{2}\sigma)]\} \tag{19}$$

where

$$Q_7 = (q_{17}q_{s7})^{1/2}\exp(\tfrac{7}{8}\beta tA)\cosh[\beta(\tfrac{7}{8}A - B) + \tfrac{1}{2}\ln(q_{17}/q_{s7})]$$
$$Q_8 = (q_{18}q_{s8})^{1/2}\exp(\beta tA)\cosh[\beta(A - B) + \tfrac{1}{2}\ln(q_{18}/q_{s8})].$$

Carrying out a similar transformation but with respect to the two terms in braces on the right-hand side of formula (19), we obtain

$$I = 4(Q_7Q_8)^{1/2}\cosh[\beta(D - \tfrac{1}{2}\sigma) + \tfrac{1}{2}\ln(Q_7/Q_8)].$$

On substituting this expression into formula (17) and inserting the resulting expression into relationship (11), we finally derive the thermodynamic potential Ω in the form

$$\Omega = \Omega_0 + \tfrac{1}{2}N\sigma + \tfrac{1}{2}NG\langle\xi\rangle^2 - TN\ln[4(Q_7Q_8)^{1/2}] - TN\ln\{\cosh[\beta(D - \tfrac{1}{2}\sigma) + \tfrac{1}{2}\ln(Q_7/Q_8)]\}. \tag{20}$$

From formula (10) we then obtain

$$c = \tfrac{1}{2}\{1 + \tanh[\beta(D - \tfrac{1}{2}\sigma) + \tfrac{1}{2}\ln(Q_7/Q_8)]\}. \tag{21}$$

Thermodynamic potential (20) describes the system in terms of the chemical potential σ. If we are interested in the case of a fixed concentration c, then the thermodynamic potential Φ, which is of the form

$$\Phi = \Omega - Nc\sigma \tag{22}$$

should be introduced. In formula (22) the value of σ must be expressed in terms of c. According to (21), we have

$$\sigma = 2D - T\ln[cQ_8/(1-c)Q_7]. \tag{23}$$

On inserting expression (20) into formula (22) and making use of expression (23) for σ, the thermodynamic potential Φ can be represented in the form

$$\Phi = \Phi_0 + \tfrac{1}{2}NG\langle\xi\rangle^2 - Nt(1 - \tfrac{1}{8}c)G\langle\xi\rangle - TN[c\ln(\cosh Y) + (1-c)\ln(\cosh Z)] \tag{24}$$

where

$$\Phi_0 = \Omega_0 + ND(1-2c) - Nt(1 - \tfrac{1}{8}c)(g_1p/K - J_1) + TN\{c\ln[c(q_{17}q_{s7})^{-1/2}] + (1-c)\ln[(1-c)(q_{18}q_{s8})^{-1/2}]\}$$
$$Y = \tfrac{7}{8}\beta(J + \tfrac{7}{8}U) + \tfrac{1}{2}\ln(q_{17}/q_{s7}) \tag{25}$$
$$Z = \beta(J + U) + \tfrac{1}{2}\ln(q_{18}/q_{s8}).$$

Note that expressions (24) and (25) may be derived by immediate calculation of the partition function in formula (11) at fixed c, though the present approach seems to be somewhat more consistent. The mean value of $\langle\xi\rangle$ is specified as a self-consistent solution of the equation

$$\langle\xi\rangle = t(1 - \tfrac{1}{8}c) + \tfrac{7}{8}c \tanh Y + (1 - c)\tanh Z \tag{26}$$

which is a direct consequence of the condition that the potential Φ in form (24) be a minimum with respect to $\langle\xi\rangle$. Relationships (24)–(26) yield the total description of the thermodynamics of the system in question at a given concentration of defective inclusions.

4. Analysis of the self-consistent solution

It is useful to rewrite equation (26) in the form

$$\tilde{T}(Z - Z_0) - \tilde{p} = (1 - c)z + \tfrac{7}{8}cy \tag{27}$$

where

$$\begin{aligned} &\tilde{p} = g_1 p/K + t(1 - \tfrac{1}{8}c) + (U - J_1)/G \\ &z = \tanh Z \qquad y = \tanh Y \\ &Y = \tfrac{7}{8}Z - W - \tfrac{7}{64}\tilde{\beta}\tilde{U} \qquad Z_0 = \tfrac{1}{2}\ln(q_{18}/q_{s8}) \\ &W = \tfrac{1}{2}\ln[(q_{s7}/q_{17})(q_{18}/q_{s8})^{7/8}] \\ &\tilde{T} = 1/\tilde{\beta} = T/G \qquad \tilde{U} = U/G. \end{aligned} \tag{28}$$

According to (1) and (2), we have $W = 0.5520$ and $Z_0 = 3.4217$. Equation (27), containing a linear function of Z on the left-hand side, is a modification of the classical matching condition on the order parameter in molecular-field theory [6, 8]. The terms with z and y on the right-hand side of equation (27) can be connected with the change in state of perfect and defective inclusions, respectively. So, the right-hand side of (27) as a function of Z is roughly speaking a step function with either one step or two steps depending on the value of Y. In the latter case the part between the steps is responsible for the intermediate phase, in which both the molten states of perfect inclusions and the solid states of inclusions with a vacancy are predominant. Note that inasmuch as $W > 0$ and the condition $U > 0$ seems to be plausible in the adopted model, the other type of intermediate state corresponding to the combination of the solid states of perfect inclusions and the liquid states of defective ones is forbidden. This statement follows immediately from the fact that, according to (28), a point of inflection of y as a function of Z occurs at $Z > 0$.

If there are several solutions of equation (27) simultaneously, then the stable one apparently corresponds to the minimum value of thermodynamic potential (24). The condition that the straight line representing the linear function on the left-hand side of equation (27) is a tangent to the curve describing the right-hand side of the same equation is responsible for the appearance of a new solution and is of the form

$$\tilde{T} = (1 - c)(1 - z^2) + (\tfrac{7}{8})^2 c(1 - y^2). \tag{29}$$

Thus, the joint solution of equations (27) and (29) specifies spinodals, i.e. boundaries of absolute instability of metastable phases on the phase diagram.

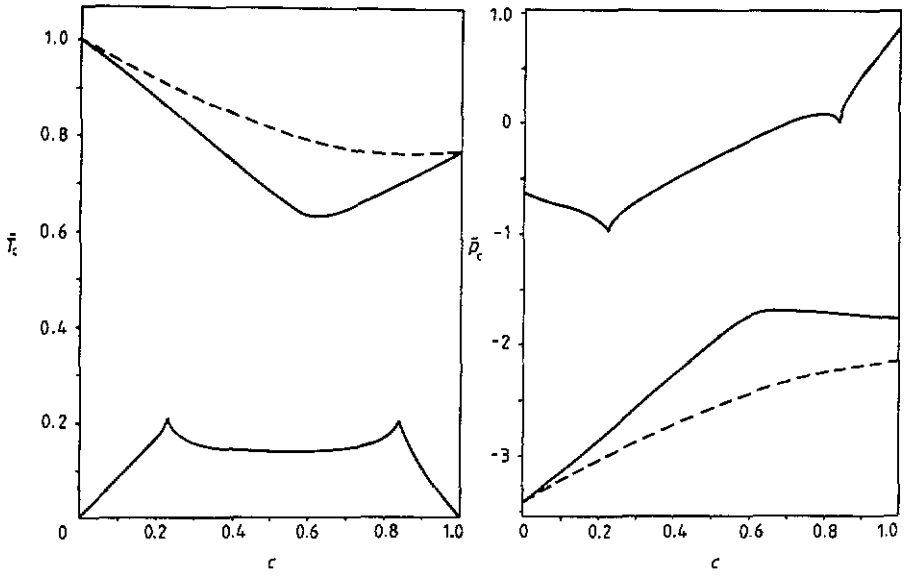

Figure 3. Parameters $\tilde{T}_c$ and $\tilde{p}_c$ of critical points versus the concentration c of defective inclusions at $\tilde{U} = 3$. The correspondence between $\tilde{T}_c$ curves and $\tilde{p}_c$ curves is obvious. The broken curves represent the case of $\tilde{U} = 0$ for comparison.

The points of inflection of the expression on the right-hand side of equation (27) as a function of Z are responsible for the singularities of the solution and are in turn determined by the relationship

$$(1 - c)(z - z^3) = -(\tfrac{1}{8})^3 c(y - y^3). \tag{30}$$

The joint solution of equations (27), (29) and (30) describes the critical points, at which spinodals converge and steady-state phase transition lines may terminate on the phase diagram. Such singularities are typical for the discussed model of isomorphic phase transitions [6].

The topology of curves describing the behaviour of the coordinates $\tilde{T}_c$ and $\tilde{p}_c$ of critical points as functions of the concentration c depends essentially on the value of $\tilde{U}$, as shown in figures 3–5. So, if $\tilde{U} = 0$, the solution for $\tilde{T}_c$, as well as for $\tilde{p}_c$ is described by a single monotonic curve. Significant bending of this curve arises upon enhancing $\tilde{U}$. Furthermore, another curve appears in the range of small $\tilde{T}_c$, when $\tilde{U}$ becomes non-zero. The cusps are typically singular points for that curve (figure 3). These cusps move towards the area of bending of the other curve upon increasing $\tilde{U}$.

In the process of increasing the value of $\tilde{U}$, the point of maximal bending of the initial curve transforms to the vertex of an angle. This event happens when the points of the maximum for both sides of equation (30) coincide at

$$z = -y = (3)^{-1/2}.$$

The appropriate values of the parameters are described by the row with $m = 1$ in table 1. At larger values of $\tilde{U}$, the vertex of an angle transforms to the point of intersection of two independent curves terminating at new cusps linked by some additional curve, as shown in figure 4. In general, all the cusps at hand are determined by the condition that

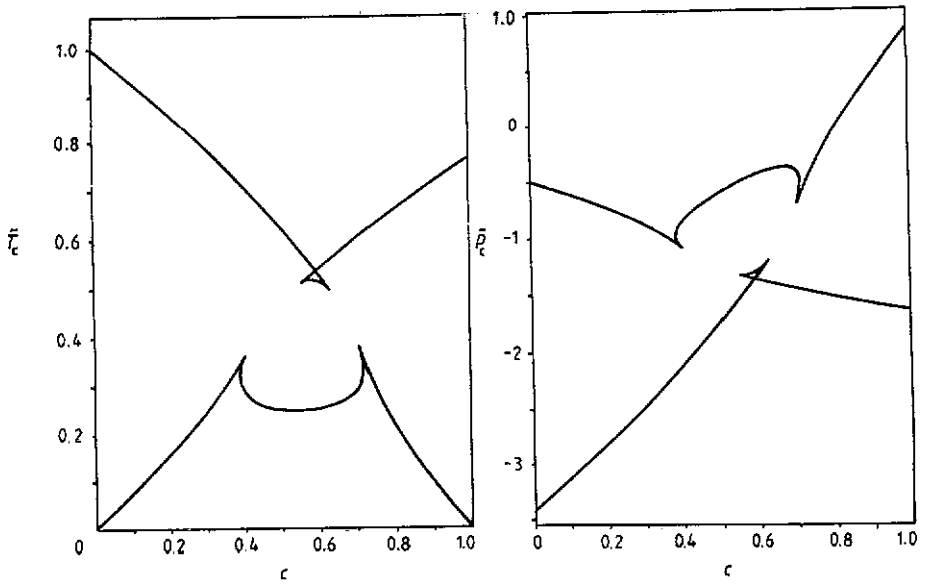

Figure 4. Dependences of $\tilde{T}_c$ and $\tilde{p}_c$ on the concentration c at $\tilde{U} = 4$.

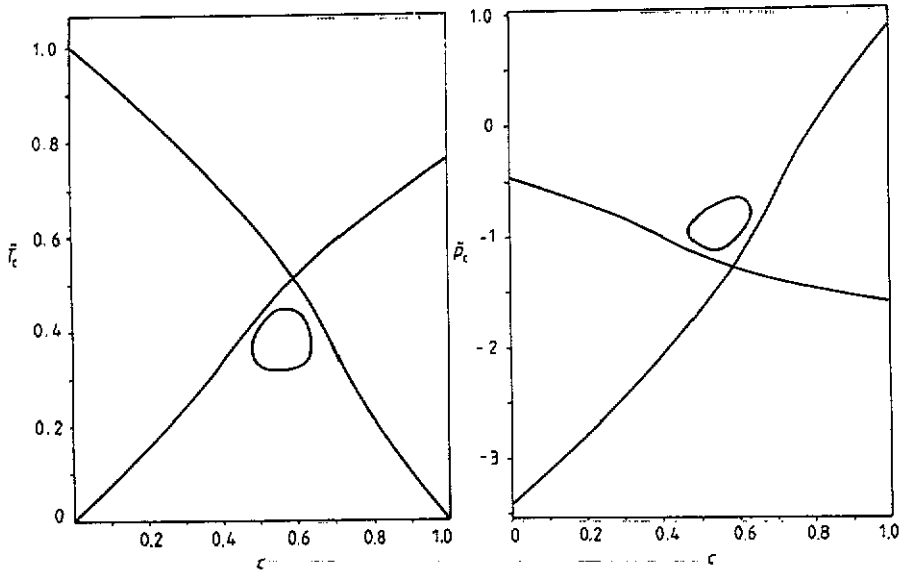

Figure 5. Parameters $\tilde{T}_c$ and $\tilde{p}_c$ as functions of the concentration c at $\tilde{U} = 4.3$.

the curves representing both sides of equation (30) as functions of Z are tangent to one another. This condition can be written as follows:

$$(1 - c)(1 - 4z^2 + 3z^4) = -(\tfrac{7}{8})^4 c(1 - 4y^2 + 3y^4). \tag{31}$$

Each cusp of one curve moves towards the appropriate cusp of the other one in the

Table 1. Parameters of the singular points labelled by number m, at which the topology of the diagram of critical points changes.

m	$\tilde{U}$	c	$\tilde{T}_c$	$\tilde{p}_c$
1	3.5768	0.5988	0.5731	−1.5127
2	4.0015	0.5515	0.5077	−1.3336
3	4.0702	0.6566	0.4487	−1.0086
4	4.3986	0.5592	0.3813	−0.8995

process of increasing $\tilde{U}$. The confluence of each of the above pair of cusps, which leads to their annihilation, corresponds to the vanishing of the discriminant of equation (31) regarded as a biquadratic equation with respect to either y or z. The parameters of the corresponding points are given by the rows with $m = 2$ and $m = 3$ in table 1. The annihilation of the cusps is accompanied by the splitting of the appropriate curves. As a result, a loop is formed, as shown in figure 5.

Further increase in the value of $\tilde{U}$ gives rise to some deformation of the intersecting curves without any essential change in their mutual arrangement. As far as the loop is concerned, its size reduces down to zero, so that there is a point at which the loop collapses. To determine the parameters of the latter point, the following derivative should be considered:

$$\frac{d\tilde{T}_c}{dc} = \frac{\frac{48}{64}(1-y^2) - (1-z^2)}{1 + \frac{343}{2048}(y-y^3)\tilde{U}\tilde{T}_c^{-2}}. \tag{32}$$

Expression (32) is obtained as a result of differentiating equation (29), with formula (30) taken into account. If both the numerator and denominator of the expression on the right-hand side of equation (32) are equal to zero, then the value of that derivative is indefinite. But this is just the case corresponding to the point of interest. The appropriate parameters are described by $m = 4$ in table 1.

As far as the choice of the thermodynamic variables of the phase diagram is concerned, the definition of the introduced parameter $\tilde{p}$ includes a regular term dependent on c. This simplifies the above analysis, but the topology of the dependences discussed here is not changed radically.

Typical patterns of the phase diagram on the $(\tilde{p}, \tilde{T})$ plane at a fixed concentration are plotted in figure 6. The characteristic distinction of the critical points that are regarded as being supplementary ones, which are described either by the curves linking the cusps or by the loop, follows from the figure. Indeed, only the spinodals converge and terminate at these critical points as shown in figure 6(a). In this case there are also three phase transition lines connected with the intermediate phase. Two of them are in the region of metastability adjoining $\tilde{T} = 0$ and the third line terminates at the critical point depicted at the bottom of the inset. However, all these lines are interrupted by the spinodals and do not arrive at the critical points in question. The behaviour of the supplementary critical points is determined by the singularities of the curves in figures 3–5. In particular, the vertical slope of these curves specifies the confluence of the critical points in question, so that the topology of spinodals changes to the form shown in figure 6(b). On the other hand, if we deal with the cases given in figures 3 and 4, the multivalued character of the solution for the spinodals shown in the inset of figure 6(a) is lost at the cusps mentioned above.

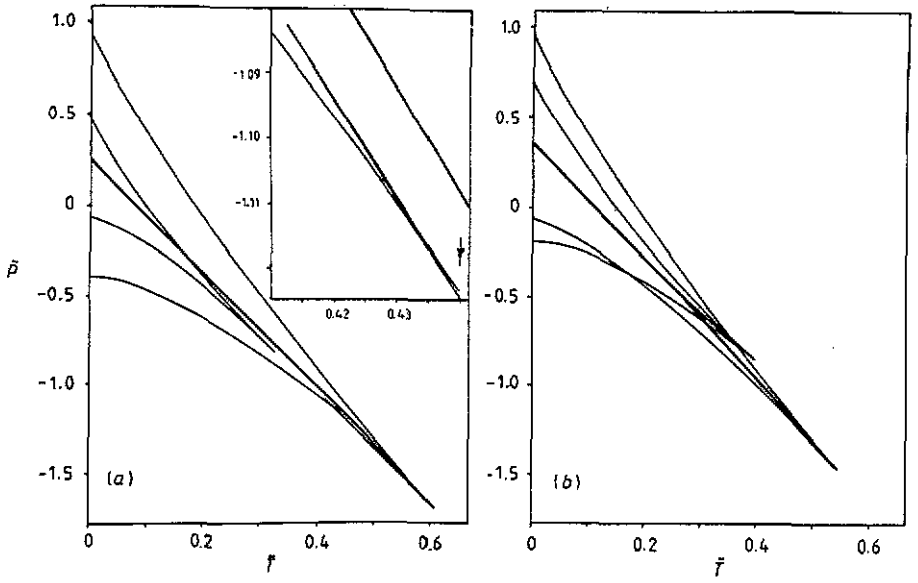

Figure 6. Phase diagrams on the pressure–temperature plane at $c = 0.5$ for either (*a*) $\tilde{U} = 4.3$ or (*b*) $\tilde{U} = 6$. The heavy curves are steady-state phase transitions, the thin curves are spinodals. The region of many-valued solutions near the lower spinodal (*a*) is shown in the inset. Here the single heavy curve at the top describes the steady-state phase transition, and the arrow points out the critical point at which the line of equilibrium between the two metastable phases terminates. The triple point at $\tilde{T}_t = 0.2770$, $\tilde{p}_t = -0.5197$ is a peculiarity of diagram (*b*). The lines restricting the intermediate phase as a stable one converge at this point from the side of larger $\tilde{T}$.

Another important consequence is associated with the fact that in general one of the two critical points at which the lines of the steady-state phase transitions terminate occurs at a lower temperature. As a result, this critical point may be easily observable in the region of stability (figure 6(*b*)) or it lies in the region of metastability as shown in figure 6(*a*). The motion of this critical point towards the region of stability happens on enhancing $\tilde{U}$. It is essential that the triple point arises on the phase diagram when the critical point in question becomes stable. At the triple point three phase transition lines separating all three admissible phases of the system converge. Upon further increasing $\tilde{U}$, the position of the triple point goes towards zero temperature. At the moment when the triple point arrives at zero temperature, the total splitting of the phase transition lines separating the intermediate phase appears. The region of the parameters $\tilde{U}$ and c where the triple points exist is drawn in figure 7. The point of singularity c_1, which is essential there, is described by the parameters with $m = 1$ in table 1.

The value c_1 is the boundary concentration between the regions of predominant influence of either perfect inclusions or defective ones. Both the examples in figure 6 elucidate the case of $c < c_1$. In the event of $c > c_1$, the form of the phase diagram on the $(\tilde{p}, \tilde{T})$ plane changes in such a way that the stable critical point at a lower temperature lies below the steady-state line of the other phase transition, whereas the metastable positions of this point are located above that line.

In general, we see that in the region of small $\tilde{U}$, where there is no triple point, the phase transition of melting in the adopted system of the two types of inclusions happens

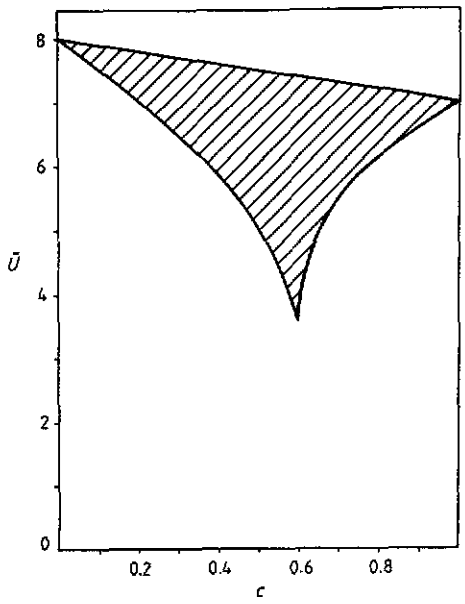

Figure 7. Regions of the $(\tilde{U}, c)$ plane where the different types of phase diagrams exist. There is a triple point in the hatched area. In the lower part there is a single line of the steady-state phase transition between the totally liquid and solid phases. At the top of the diagram there are two independent lines restricting the region of stability of the intermediate phase.

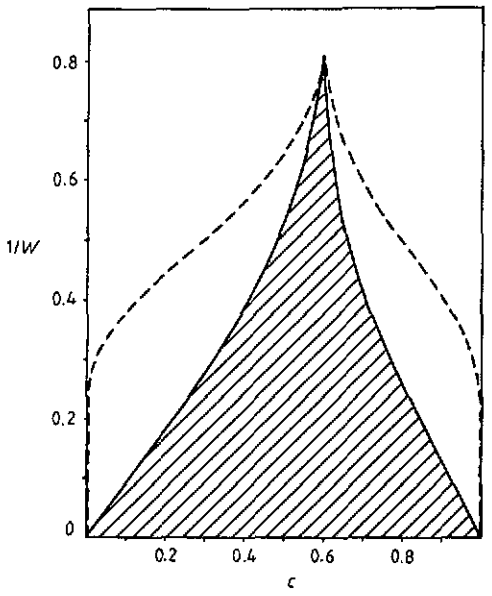

Figure 8. Hatched area gives the region of stability of the intermediate phase at $\tilde{U} = 0$ if the variation of the value of W is admissible. The broken curves restrict the region of existence of the intermediate phase.

to be eutectic. In the case of a triple point the eutectic region occurs at temperatures below the temperature of that triple point. Finally, if

$$\tilde{U} > 8 - c$$

then the eutectic region is absent.

For the sake of completeness of our analysis of the possibilities that originate from equation (27), we also point out the typical changes of the phase diagram as a function of W at $\tilde{U} = 0$, though this situation, strictly speaking, lies beyond the scope of the concrete model representation of local melting proposed in the present paper. At this stage of the discussion it is in order to point out that W has a purely statistical nature in conflict with $\tilde{U}$ whose nature is dynamic. The appearance of the two-step character of the expression on the right-hand side of equation (27) as a function of Z is possible upon increasing W as well. In this case the second critical point is certainly created on a spinodal, i.e. in the region of metastability in accordance with the above results. Upon further enhancing W, the new critical point also goes towards the region of stability so that the triple point arises in the same manner. The regions of the different types of behaviour are shown in figure 8. The singular character of the boundary curves also manifests itself at $c = c_1$. It is worth noting that the supplementary critical point, at which only spinodals terminate and which moves towards zero temperature for increasing W,

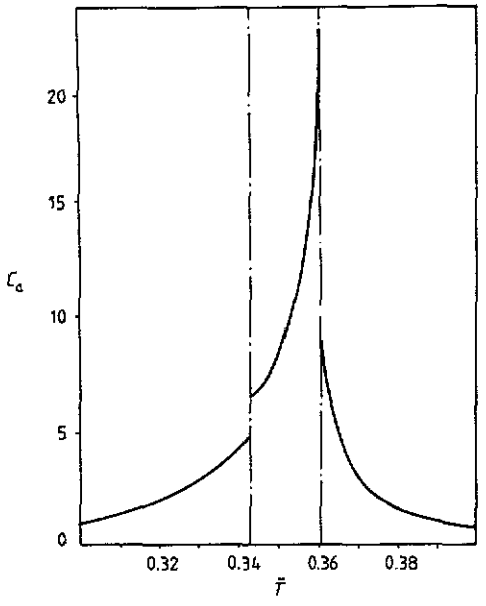

Figure 9. Anomalous part C_a of the specific heat versus the temperature $\tilde{T}$ in the vicinity of the phase transitions indicated by the chain lines. The case of $\tilde{U} = 6$, $c = 0.5$, $\tilde{p} = -0.75$ is considered.

does not arrive at zero temperature at finite values of W. This fact follows from the non-zero slope of a plot corresponding to the expression on the right-hand side of relationship (27) as a function of Z at finite values of Z. As a result, the triple point, if it appears, always occurs at a finite temperature there.

5. Discussion

Apart from the general analysis of the phase diagram, it seems to be instructive to consider the behaviour of the specific heat as a rather informative thermodynamic characteristic. According to (15) and (24)–(26), the derivative of Φ with respect to temperature is calculated. As a result, the anomalous part of the specific entropy corresponding to the phase transition in question can be written in the form

$$S_a = c\ln(\cosh Y) + (1-c)\ln(\cosh Z) + \tfrac{7}{64}c\tilde{U}y/\tilde{T} - (Z - Z_0)[\tilde{T}(Z - Z_0) - \tilde{p}]. \tag{33}$$

On differentiating expression (33) with respect to temperature and making use of the value of $\mathrm{d}Z/\mathrm{d}\tilde{T}$ derived from relationship (27), we obtain

$$C_a = \frac{\tilde{T}^2[Z - Z_0 - \frac{49}{512}(c\tilde{U}/\tilde{T}^2)(1-y^2)]^2}{\tilde{T} - (1-c)(1-z^2) - \frac{49}{64}c(1-y^2)} + \tfrac{49}{4096}(c\tilde{U}^2/\tilde{T}^2)(1-y^2) - \tilde{T}(Z-Z_0)^2.$$

In the case of the phase transition with the intermediate phase, the temperature behaviour of C_a is shown in figure 9. The mutual proximity of both the phase transitions, which is specific in this particular case, manifests itself in the monotonic increase of that branch

of the overall C_a curve that is situated between the phase transitions. A minimum point of that branch exists but lies in the region of metastability. At higher $\tilde{U}$ the minimum point of interest tends to the region of stability of the intermediate phase. As a result, we return to the usual singularities of the heat capacity, which are characterized by increasing magnitude on both sides of each phase transition point [3].

Note that the common deformation nature of both the energies of the different states of a single inclusion and the energy of the indirect interaction via an elastic matrix may be regarded as a parametric feature of the above model. As a result, the typical energy parameter G of the system is determined by the set of elastic energies each of which is large enough in comparison with melting temperatures observed experimentally. The required smallness of the value of G compared with the elastic energies follows from the form of the appropriate dependence given by (13) and is a result of several circumstances. First of all, the elasticity of an included material leading to an estimate of g_1 should obviously be less than the elasticity of the host matrix determined by the parameters λ and μ. The presence of a difference between the inverse values of the elastic moduli is one more origin for the reduction of the value of G. Finally, according to (4), the value of g_1 itself is specified by the difference between the elastic parameters of an atom in the liquid and solid states. The latter is exclusively important inasmuch as a non-zero value of that difference turns on the present mechanism of melting. Hence, the non-zero effect can immediately be connected with the non-linear dependence of the energy of an atom in the molten state on the strong deformation, in accordance with the geometry of our model representation.

To estimate the numerical values of the parameters involved above, we consider clusters composed of eight indium atoms and embedded in a zeolite matrix. Such a situation corresponds to experiment [1]. According to [3], at $c = 0$ we directly obtain $G = 9 \times 10^{-20}$ J, $\tilde{T} = 0.33$ and $\tilde{p} = -1.15$. On setting $E = 3 \times 10^{-13}$ N m^{-2} and $\sigma = 0.1$ for Young's modulus and Poisson's ratio of the elastic matrix, respectively, as well as $v = 1.9 \times 10^{-27}$ m^3 [9], from expression (13) for G, we derive $g_1 = 2 \times 10^{-18}$ J. The value of g_1 can be connected with the relative atomic deformation

$$u = 1 - (r_l/r_s)^3 = 0.24$$

where r_l and r_s are the model atomic radii in the liquid and solid states, respectively. We make use of the approximation

$$g_{al} - g_{as} = Bu + \tilde{B}u^2$$

where the linear dependence of the atomic elasticity on the deformation is taken into account. On putting $B = 1.1 \times 10^{-18}$ J as a value typical for indium [10], we obtain $\tilde{B} = 3.9 \times 10^{-18}$ J. We can also write

$$E_a = Bu^2/2 + \tilde{B}u^3/3$$

and, therefore, according to (4), we have $J_1/G = 20$. On the other hand, the values of the parameters mentioned above give rise to the relationship $\tilde{U} = 0.7t$. On substituting the obtained estimates into the expression for $\tilde{p}$ in set (28), at $p = 0$ we find $\tilde{U} = 7.9$, $g_{as} = 2.6 \times 10^{-18}$ J and $g_{al} = 3.1 \times 10^{-18}$ J. That value of $\tilde{U}$ specifies the character of the expected peculiarities of the solution upon changing the concentration c in the case of the experimental system [1]. As far as the physical nature of the value of g_{as} is concerned, it would be associated with stressed states of solid inclusions [9], though the real origin of that stress may be the distortion of interatomic bonds due to the fact that the geometry

of the atomic configuration of a cluster differs drastically from the typical atomic configuration of bulk indium [10].

It is worth pointing out the model peculiarities of the results obtained as far as the picture of melting is concerned. First of all, the configuration of the molten state can be somewhat different in real objects. Nevertheless, the large entropy effect typical for the experimental phase transition of melting [11] agrees with the present model. This circumstance enables us to hope that adequate orders of magnitude of the involved parameters are obtained here. The statement that there is intimate elastic contact of an inclusion in the solid state with the surrounding matrix is essential here. Of course, the other situation when a solid inclusion exists freely in a cavity is also possible. The appropriate complication reduces to some increases in the values of q_{s8} and q_{s7} as well as to the requirement that $g_{as} = 0$. The appearance of some threshold pressure p_{th}, at which elastic contact of an inclusion with the matrix is recovered, can be expected as well. Moreover, in this case the statistical contribution of the rotational degrees of freedom of a solid inclusion as a whole should also be taken into account. Strictly speaking, the latter contribution would already be calculated in the considered case, provided that cavities are perfectly spherical. However, the absence of this effect, at least in some real systems, seems to be plausible due to the fact that the cavities in question are not absolutely spherical. As a result, definite orientations of inclusions should be energetically favourable.

Note that the effects of crystalline anisotropy and possible anisotropy of elastic deformation of the medium connected with the dynamical influence of many-body inclusions have been ignored because they do not change the obtained results qualitatively. Indeed, the appropriate contributions of dipole and short-range forces are small compared with the discussed effect of the mean field [3, 12].

The general picture of melting can also be more complicated owing to the possibility of the existence of some premelting states of inclusions [2]. As a result, the phase diagrams discussed here can be modified by features investigated in detail in [3].

It is instructive to note that the present phenomenon yields the important pattern of thermodynamics with critical points, which are not widespread in solids. The principal possibility of exploring the vicinities of the above critical points by means of changing the concentration of defective inclusions is confirmed by experimental results [13] (see also [14]).

The analysis accomplished in the present paper shows that, even in the simplest case of only two kinds of inclusions, the task contains a lot of essential parameters, so that an experimental check of the obtained results over a wide range of values of the parameters seems to be quite difficult. Nevertheless, variation of the material of the inclusions can lead to some change in the value of $\tilde{U}$. Variation of the concentration of defective inclusions can be achieved by the choice of the conditions under which the synthesis of given composites is performed. Appropriate thermodynamic investigations under pressure are desirable as well. As far as the possibility of a more complicated experimental situation dealing with a larger number of different types of inclusions is concerned, the results mentioned above could also be useful as grounds for classification of miscellaneous types of thermodynamic behaviour. In particular, it is important for the understanding of complex eutectics typical of many-component composites. The structural picture of local melting proposed in the present paper is one more essential subject of interest. In our opinion, thorough experimental verification of the predicted thermodynamic behaviour would be extremely useful for developing representations of the phenomenon of melting as a whole.

Note that all the above calculations are based on the exactly soluble model, which enables us to perform them with sufficient accuracy. The principally novel types of phase diagram predicted here increase our knowledge about the possible character of isomorphic phase transitions. As far as the ferroelastic interaction leading to the collective effect of transformation of local states is concerned, that interaction seems to be universal in elastic solids. Because of the latter, we believe that our results are applicable to a wide circle of phase transitions taking place in compounds that consist of several sorts of two-level systems. The numerical values describing the relations between the energies and degrees of degeneracy are to be corrected herein.

References

[1] Alekseev Yu A, Bogomolov V N, Egorov V A, Petranovskii V P and Kholodkevich S V 1982 *Zh. Eksp. Teor. Fiz. Pis.* **36** 384 (1982 *Sov. Phys.–JETP Lett.* **36** 463)
[2] Kholopov E V 1986 *Fiz. Tverd. Tela* **28** 1265 (1986 *Sov. Phys.–Solid State* **28** 714)
[3] Kholopov E V 1987 *J. Stat. Phys.* **48** 215
[4] Kholopov E V 1987 *Preprint* IIC 87-14, Institute of Inorganic Chemistry, Novosibirsk
[5] Landau L D and Lifshitz E M 1986 *Theory of Elasticity* (Oxford: Pergamon) ch 1
[6] Kholopov E V 1979 *Zh. Eksp. Teor. Fiz.* 77 293 (1979 *Sov. Phys.–JETP* **50** 151)
[7] Kholopov E V 1979 *Phys. Lett.* A **73** 377
[8] Brout R 1965 *Phase Transitions* (Amsterdam: Benjamin) ch 2
[9] Alekseev Yu A, Bogomolov B N, Zhukova T B, Petranovskii V P and Kholodkevich S V 1982 *Fiz. Tverd. Tela* **24** 2438 (1982 *Sov. Phys.–Solid State* **24** 1384)
[10] Kittel C 1971 *Introduction to Solid State Physics* (New York: Wiley) chs 1, 4
[11] Bratkovskii A M, Vaks V G and Trefilov A V 1984 *Zh. Eksp. Teor. Fiz.* **86** 2141 (1984 *Sov. Phys.–JETP* **59** 1245)
[12] Kholopov E V 1981 *Phys. Lett.* A **85** 363
[13] Bogomolov V N, Kolla E V and Kumzerov Yu A 1985 *Zh. Eksp. Teor. Fiz. Pis.* **41** 28 (1985 *Sov. Phys.–JETP Lett.* **41** 34)
[14] Kholopov E V 1987 *Fiz. Tverd. Tela* **29** 2298 (1987 *Sov. Phys.–Solid State* **29** 1324)